IEEE Access
Multidisciplinary | Rapid Review | Open Access Journal

Received April 24, 2018, accepted June 11, 2018, date of publication June 28, 2018, date of current version July 30, 2018.

Digital Object Identifier 10.1109/ACCESS.2018.2851282

A Robust Sparse Representation Based Pattern Recognition Approach for Myoelectric Control

YANJUAN GENG[1,2], (Member, IEEE), YATAO OUYANG[3], OLUWAROTIMI WILLIAMS SAMUEL[1,2], (Member, IEEE), SHIXIONG CHEN[1,2], (Member, IEEE), XIAOQIANG LU[4], (Senior Member, IEEE), CHUANG LIN[1,2], AND GUANGLIN LI[1,2], (Senior Member, IEEE)

[1]Shenzhen Institutes of Advanced Technology, Chinese Academy of Sciences, Shenzhen 518055, China
[2]Key Laboratory of Human-Machine Intelligence-Synergy Systems, Chinese Academy of Sciences, Shenzhen 518055, China
[3]Guangdong Provincial Work Injury Rehabilitation Center, Guangzhou 510440, China
[4]Xi'an Institute of Optics and Precision Mechanics, Chinese Academy of Sciences, Xi'an 710119, China

Corresponding authors: Chuang Lin (chuang.lin@siat.ac.cn) and Guanglin Li (gl.li@siat.ac.cn)

This work was supported in part by the National Natural Science Foundation of China under Grant U1613222 and Grant U1613228 and in part by the Shenzhen Basic Research Grants under Grant JCY20160331185848286.

ABSTRACT Interferences in the form of white Gaussian noise (WGN) are inevitable during long-term electromyogram (EMG) recordings. Even with the aid of advanced signal denoising techniques, such an intermittent interference is hardly detected and attenuated in the practical use of EMG-driven control systems. Hence, a robust pattern recognition scheme that is invariant to noise contamination would potentially aid the realization of an efficient EMG-based pattern recognition (EMG-PR) control system. To this end, an EMG-PR scheme driven by sparse representation-based classification (SRC) algorithm and root mean square (rms) descriptor (RMS-SRC) is proposed in this paper. The accuracy and the robustness of the proposed scheme were investigated using the high-density surface EMG recordings from 12 traumatic brain-injured patients and 5 post-stroke survivors. For benchmark comparison, another three different feature sets and four pattern recognition algorithms were considered. The optimal pattern recognition schemes with respect to each feature-classifier combination were first selected in the absence of WGN contamination. Then, six levels of WGN with a signal-to-noise ratio (SNR) ranging from 5 to 30 dB were added into the EMG recordings, respectively, to mimic the different WGN interferences. Our result showed that the proposed RMS-SRC scheme could achieve a similar accuracy with the benchmark schemes in the presence of limited noise contamination (0–15 dB), and significantly outperformed the other schemes when the SNR of WGN increased (20–30 dB). More notably, the RMS-SRC scheme significantly outperformed the other pattern recognition schemes when the WGN existed in either training set or testing set only. The findings proved the comparative advantage of the proposed RMS-SRC pattern recognition scheme over the other currently used schemes in the myoelectric control. Thus, the proposed scheme would potentially facilitate the development of EMG-driven rehabilitation robots for accurate and dexterous assistive training for patients with neurological disorders.

INDEX TERMS Electromyogram, pattern recognition, sparse representation classifier, robustness, white Gaussian noise.

I. INTRODUCTION

Dozens of recent studies have reiterated the potential of electromyogram (EMG) pattern recognition (EMG-PR) technique in providing intuitively dexterous myoelectric control system that is capable of supporting multiple degrees of freedom (DOFs) functions. To that end, EMG-PR based prostheses control strategy has been extensively investigated in the last two-three decades with a number advancement reported in literature [1]–[3]. Due to its promising nature, EMG-PR techniques have recently been applied to control rehabilitation robots for assistive motor training for patients with motor impairment resulting from neurological disorders [4]–[11]. It should be noted that during long-term EMG recordings, interferences in the form of white Gaussian noise (WGN)

are inevitable due to electromagnetic interference, internal noise of operational amplifier, and thermal noise of electronic elements. Moreover, the variation of electromagnetic interference would lead to the change of WGN, and that's why it becomes difficult to be detected in the practical use of EMG-driven systems. For an EMG-PR system in which the good repetition of EMG patterns is highly demanding, varying WGN interference would lead to poor characterization of the EMG patterns associated with the individual's limb motion intent, and thus degrade the performance of myoelectric control system.

To obtain high quality EMG recordings, different signal denoising techniques have been proposed and applied. Among these denoising approaches, the conventional IIR and FIR digital filters are commonly used to attenuate power line frequency interference as well as DC components in the EMG recordings [12]. However, these filters are found to be inappropriate for eliminating WGN that are inevitably associated with long-term usage of EMG recording systems. This is because the frequency components of WGN usually overlap with most of the useful EMG frequency bands. Other advanced filtering techniques such as adaptive filtering, nonlinear filtering, and spectral enhancement approaches have been utilized to optimally preserve the useful EMG components through maximum attenuation of the WGN contamination [13]–[16]. Additionally, different variants of spatial filtering techniques have been utilized to remove dominant noise components in multi-channel EMG recordings, thus enhancing the separation property of EMG signals and improving the performance of EMG-PR systems [17], [18].

It is noteworthy that most of the abovementioned signal preprocessing methods were intended for offline analysis only due to their large computational cost, and it becomes challenging for these complex denoising methods to be used in real-time EMG-PR control systems. Therefore, adopting a robust pattern recognition scheme that is invariant to noise contamination might be an alternative way to achieve efficient EMG-PR control system.

According to recent literatures, a couple of efficient EMG features have been proposed to enhance the robustness of EMG-PR system [19], e.g., the time-dependent spectral features invariant to limb position change [20], the frequency-domain features and temporal-spatial descriptors robust to different muscle contraction force [21], [22]. However, only a few studies have investigated the robustness of EMG features in terms of their tolerance to noise [23]. On the other hand, an increasing array of pattern recognition algorithms such as artificial neural networks (ANN) [24], linear discriminant analysis (LDA) [10], [25], [26], k-nearest neighbor (KNN) [10], [27], Gaussian mixture model (GMM) [28], fuzzy logic [29], [30], random forest (RF) [31], [32], and support vector machine (SVM) [33] were proposed in the last four decades. It should be noted that most of these studies focused on the discriminative capability of the methods with scarce investigation on the robustness of EMG-PR scheme especially to WGN contamination to date.

Aiming at developing EMG-PR control system that is robust to noise with accurate and stable performance, a pattern recognition scheme driven by sparse representation based classifier (SRC) and root mean square (RMS) feature denoted as RMS-SRC is proposed in this study. The SRC has been extensively used for face recognition because of its high accuracy, which might be attributed to the collaborative representation of SRC algorithm [34]. Moreover, the SRC has been proved to be robust to image occlusion and corrupted data because these factors are often sparse with respect to the standard (pixel) basis [35]–[37]. In this study, we hypothesize that SRC may also be a potential pattern recognition algorithm for myoelectric control systems. For benchmark comparison, the performances of commonly adopted feature-classifier combinations were studied under different conditions alongside the proposed RMS-SRC scheme. More precisely, three different feature extraction methods in addition to RMS and four widely applied pattern recognition algorithms including LDA, KNN, RF, and SVM were considered. To that end, the accuracy and stability of the proposed RMS-SRC scheme was firstly assessed in comparison with the other feature-classifier combinations. Subsequently, the robustness of the proposed scheme to noise interference was evaluated. The proposed RMS-SRC scheme may potentially facilitate the realization of accurate, stable, and robust control systems for EMG-driven rehabilitation robots to administer effective assistive training to patients with neurological disorders.

II. METHODS

A. SUBJECTS

A total of 17 mildly-impaired patients consisting of 12 with traumatic brain injury (TBI) and 5 with stroke (ST) participated in the study. Overall, there were 3 female and 14 males, with an average age of 38.5 $\pm$ 13.5 years old across all subjects. According to an objective evaluation by a physiotherapist, the recruited patients were in the stage IV-VI based on the Brunnstrom Assessment Scale and got scores of 35-61 on the Fugl-Meyer Assessment of Sensorimotor Recovery after stroke, in which a zero score denotes no function and a score of 66 represents normal function. The subjects reported that it is their first time to participate in this kind of research study. After proper explanation of the aim of the study, the subjects agreed to participate in the study. They further gave written informed consent and provided permission for the publication of their photographs and data for scientific and educational purposes. The study was conducted in accordance with the protocols approved by the Research Ethics Board of the Shenzhen Institutes of Advanced Technology, Chinese Academy of Sciences.

B. EXPERIMENT AND DATA PREPROCESSING

During the experiment, each subject was asked to perform 21 different forearm and hand movements in addition to the

no movement limb task as described in FIGURE 1. The number of observed movements for each subject varied due to their different levels of motor ability/impairment. Each movement was maintained for about 6 s with a moderate muscle contraction force (50%-70% of the maximum contraction force) and repeated 6 times per trial, and a rest period of about 8 s was observed between two successive isometric contractions in trial.

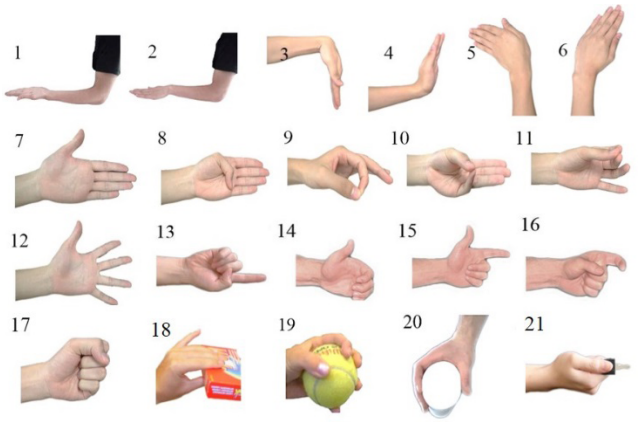

FIGURE 1. 21 Forearm and hand movements.

The High-density EMG (HD-EMG) acquisition system (Refa-128, TMS International BV, Netherlands) was used to record the EMG signals with the former 56 monopolar electrodes each having a diameter of 5mm. The electrode placement on the forearm and hand of each subject is shown in FIGURE 2. After pre-examining the arms of the subjects, 48 of the 56 HD-EMG electrodes were placed on subjects' forearm muscles in an 8 × 6 grid, specifically, located from 1cm proximal to elbow crease to 1/3 distal to wrist joint with an inter-electrode distance of around 2 cm. Meanwhile the remaining eight electrodes were placed on the hand muscles with two electrodes on the first dorsal interosseous, three on the thenar muscles, and three on the hypothenar muscles. Afterwards, a reference electrode was fixed on a nylon bracelet and worn on each subject's wrist. Subsequently, the myoelectric signals corresponding to all classes of movements were recorded at a sampling rate of 1024 Hz, 22 bits ADC for all the subjects.

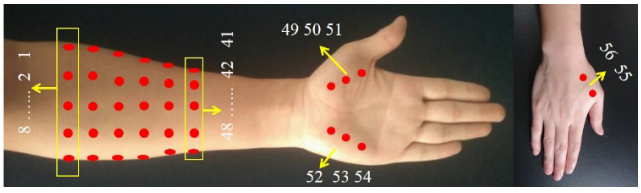

FIGURE 2. Placement of HD-EMG electrodes.

To remove the motion artifact and power-line interference, the recorded EMG signals were digitally filtered with a five-order Butterworth high-pass filter at 60 Hz. Afterwards, the active EMG data corresponding to each muscle contraction was segmented manually considering the fact that neurologically disordered subjects could not follow the prompt cues punctually in the data acquisition experiment.

C. PERFORMANCE EVALUATION PROTOCOL

To evaluate the performance of the proposed RMS-SRC scheme in terms of its accuracy and stability for limb movement intent decoding, three additional time-domain feature sets aside RMS, and four widely applied pattern recognition algorithms including LDA, KNN, RF, and SVM were considered. By including different levels of WGN (with signal noise ratio (SNR) of 5dB, 10dB, 15dB, 20dB, and 25dB, and 30dB) into the EMG recordings, the robustness of the proposed RMS-SRC scheme was assessed with respect to the optimal feature-classifier combinations obtained in the study.

1) FEATURE EXTRACTION

Before feature extraction, a shifting analysis window with a time length of 150 ms and an increment of 100 ms (50 ms overlapping) was used to segment the preprocessed EMG signals into a series of analysis windows, then each EMG feature was extracted from these segments to obtain a feature matrix for each feature extraction method. Four different previously proposed time-domain feature sets abbreviated as RMS, TD2, TD4, and TDAR were used to characterize the EMG signal patterns in each analysis window.

- RMS: is a one-dimension feature set with only RMS.
- TD2: is a two-dimension feature set including the absolute vale of the summation of square root and the absolute value of the summation of the expth root of the data in a given analysis window and its mean [38].
- TD4: is the most commonly used four-dimension feature set, including the mean absolute value, zero crossing, wave length and slope sign changes [39].
- TDAR: the combination of RMS and the latter seven coefficients of seven order autoregressive model coefficients [40].

2) NOISE CONTAMINATION

To assess the robustness of the proposed RMS-SRC to noise contamination, two noise contamination schemes were considered in current study. In the first scheme, we assumed that the WGN persistently existed, so WGN with a SNR of 5 dB, 10 dB, 15 dB, 20 dB, 25 dB, and 30 dB were added to both the training EMG recordings and the testing EMG recordings. Meanwhile, to mimic the intermittent occurrence of WGN in practical settings, the training and testing EMG recordings were separately contaminated with WGN of 5 dB, 10 dB, 15 dB, 20 dB, 25 dB, and 30 dB SNR in the second scheme.

The variation of EMG recordings after adding different levels of WGN and that without WGN was described by EMG topographic maps, which were plotted by firstly computing the average RMS obtained from all segmented windows of the 48 EMG channels distributed over the forearm muscles. Afterwards, the spline interpolation algorithm was utilized to form the contours in the topographic maps.

3) PATTERN RECOGNITION

The SRC can be considered as a generalization of popular classifiers such as the nearest neighbor (NN) and nearest subspace (NS). In NN classifies, the test sample is based on the best representation in terms of a single training sample, whereas NS classifies are based on the best linear representation in terms of all the training samples in each class. The fundamental principle of SRC is to code a testing sample as a sparse linear combination of all the training samples, and then classify the testing sample by evaluating which class leads to the minimum representation error. The operational process of SRC is described as follows:

Supposing $A_i(i = 1, 2, \ldots C)$ represent the matrix formed by the training samples of the i^{th} class, then, $A_i = \left[x_{i1}\ x_{i2}\ \ldots\ \ldots\ x_{iN_i}\right] \in R^{d\times N_i}$. And the matrix A denote the total training set with C number of classes by concatenation each class, $A = [A_1, A_2, \ldots A_C] \in R^{d\times N}, N$ is the sum of N_i samples corresponding to each class. If a test sample y belongs to the i^{th} class, it can be approximately represented as a linear combination of the training samples in the corresponding class, that is,

$$\mathrm{y} = \sum\nolimits_{j=1}^{\mathrm{N}_i} x_{ij}\mu_{ij} = A_i\mu_i \tag{1}$$

Thus, the linear representation of y can be rewritten in terms of A as $y = A\mu$, where $\mu = [0, 0, \ldots \mu_i, \ldots 0, \ldots 0] \in R^N$ is the coefficient vector whose entries are zero except those associated with the i^{th} class (current class). Hence, the goal of the sparse representation involves solving the following optimization problem:

$$\left(l^1\right)\ \hat{\mu}_1 = arg\,min\,\|\mu\|_1, \quad s.t.\ y = A\mu. \tag{2}$$

In the current study, the basis pursuit denoising algorithm (BPDN) was utilized to obtained the sparest solution $\hat{\mu}_1$. Afterwards, the test sample y was reconstructed as follows:

$$\hat{y}_i = A\delta_i(\hat{\mu}_1) \tag{3}$$

Where $\delta_i(\hat{\mu}_1)$ is a vector whose non-zero entries are the entries in μ that are associated with the current class (class i).

Subsequently, the SRC decision rule is constructed to minimize the residual error which is mathematically expressed as:

$$\gamma_i\,(y) = \left\|y - \hat{y}_i\right\|_2 = \left\|y - A\delta_i(\hat{\mu}_1)\right\|_2 \tag{4}$$

Note that: If $\gamma_k\,(y) = min_i\gamma_i\,(y)$, y is assigned to class k.

In addition to the proposed SRC, four other classification algorithms abbreviated as LDA, KNN, RF, and SVM were considered for benchmark comparison, which have been used for EMG-PR analysis in previous studies [10], [25]–[27], [31], [41], [42]. Among various previously adopted classifiers, LDA is the most applied because it exhibits a simple computational structure and yield classification results that are comparable to that of other complex classifiers such as ANN or SVM. The KNN classifier has been reported to have good tolerance for arbitrary data distribution [27], and the RF is an ensemble classifier that consist of many decision trees and outputs the class that is the mode of the classes output by individual trees [43]. RF classifier has been applied in many fields for its high accuracy and the capability to handle bad data [31], [32], [44], [45]. In the current study, the computations of RF classifier were performed with the RF-Matlab package developed by Abhishek Jaiantilal (https://github.com/jrderuiter/randomforest-matlab). As for SVM, the LIBSVM toolbox developed by Lin et al. was adopted in the current study [46], and the linear kernel function was selected based on the results of a preliminary evaluation, where the linear kernel function achieved similar classification accuracy to that of the RBF kernel function, while it require a significantly lesser computational time to build the SVM classifier.

4) CROSS VALIDATION AND PERFORMANCE METRIC

To validate the results obtained via each pattern recognition schemes investigated in this study, a five-fold cross validation data partitioning technique was adopted during the motion classification. That is, all EMG recordings were divided into five consecutive parts with equal length, one of the five parts was used as the test set while the remaining four parts were used to build the classification model in each fold. The classification accuracy commonly defined as the percentage of correctly classified samples to the total number of testing samples was computed in each fold, and the average classification accuracy over all the five folds was used as the performance metric as expressed in the following equation.

$$\textit{Classification Accuracy} = \frac{\textit{Number of correctly classified samples}}{\textit{Total number of testing samples}} \times 100\% \tag{5}$$

5) STATISTICAL ANALYSIS

To examine if there is an interaction effect of feature set and classifier, the two-way ANOVA was conducted in terms of mean classification accuracy using, and the SPSS Statistical Modeling Software (SPSS 21.0 IBM Corp., Chicago, IL). If the interaction effect was insignificant, the main effects of classifiers and feature set were further examined. Furthermore, the difference among all the selected optimal feature-classifier combinations were analyzed at each specific noise level by applying a one-way ANOVA statistical technique, and a post-hoc analysis was carried out in cases where significant difference was observed among the compared means. For each selected optimal feature-classifier combination, the variation of classification performance between two noise levels was assessed with the paired-t statistical test. In the current study, the level of statistical significance was set to p-value < 0.05. And all post-hoc comparisons and t-test were made using a Bonferroni correction factor to determine the level of significance.

III. RESULTS

A. VISUALIZATION OF THE CONTAMINATED EMG RECORDINGS

To investigate the impact of noise contamination on the classification performance of the proposed scheme, the variation of EMG recordings before and after noise contamination was assessed. FIGURE 3(A) illustrates the topographic map of EMG recordings at different levels of noise contamination (0-30 dB) for ST05 who was suffering from muscular weakness, the red color denotes higher RMS of EMG and the blue color denotes lower RMS of EMG. While FIGURE 3(B) shows the variation of EMG signal amplitude from a selected representative channel. By carefully analyzing the maps, it is found that the spatial distribution of EMG topographic map was relatively consistent when the SNR of WGN is within 15 dB, but changed considerably at noise levels greater than 20 dB. Importantly, it became difficult to discriminate the onset and offset of a movement (three repetitions of active EMG) from ''no movement'' when the SNR of WGN reached 20 dB.

B. SELECTION OF OPTIMAL FEATURE-CLASSIFIER COMBINATIONS

In the absence of WGN interference, the classification accuracy when using each of the feature-classifier combinations (RMS/TD2/TD4/TDAR - LDA/KNN/RF /SVM/SRC) was computed on individual subject basis. The statistical results with two-way ANOVA suggest that there is no evidence of interaction effect of the feature set and classifier ($p\text{-}value = 0.91$), while the following post-hoc analysis with Bonferroni correction indicates that the classifier has main effect on the classification accuracy ($p\text{-}value < 0.01$) but the feature set does not have ($p\text{-}value = 0.38$).

FIGURE 4 shows the average classification accuracy across all subjects for each feature-classifier combination. It can be seen that in comparison to other classifiers, the SRC performed the best, with the average classification accuracy of 96.94 $\pm$ 3.10% (standard deviation), 96.53 $\pm$ 3.84%, 97.51 $\pm$ 3.16%, and 97.36 $\pm$ 2.87% when using RMS, TD2, TD4, and TDAR feature sets, respectively. Moreover, the standard deviation of classification accuracy for SRC fluctuated within a small range. These outcomes suggest that the SRC has merits of high accuracy combined with each feature set.

According to the average cost time to make decision for all the SRC-based pattern recognition schemes (TABLE 1), it is found that the lower the dimensionality of the feature set is, the shorter the time consumption (computation time) would be. In particular, in comparison to TDAR-SRC, the RMS-SRC scheme achieved slightly lower classification accuracy (with decrease of 0.42%), but the average cost time for RMS-SRC is 21.72 $\pm$ 5.00 s, 15.8 s shorter than that TDAR-SRC, and the difference is significant ($p\text{-}value < 0.05$) according to the one-way ANOVA and pairwise comparison in terms of the cost time. Hence, the RMS-SRC was selected as one of the optimal feature-

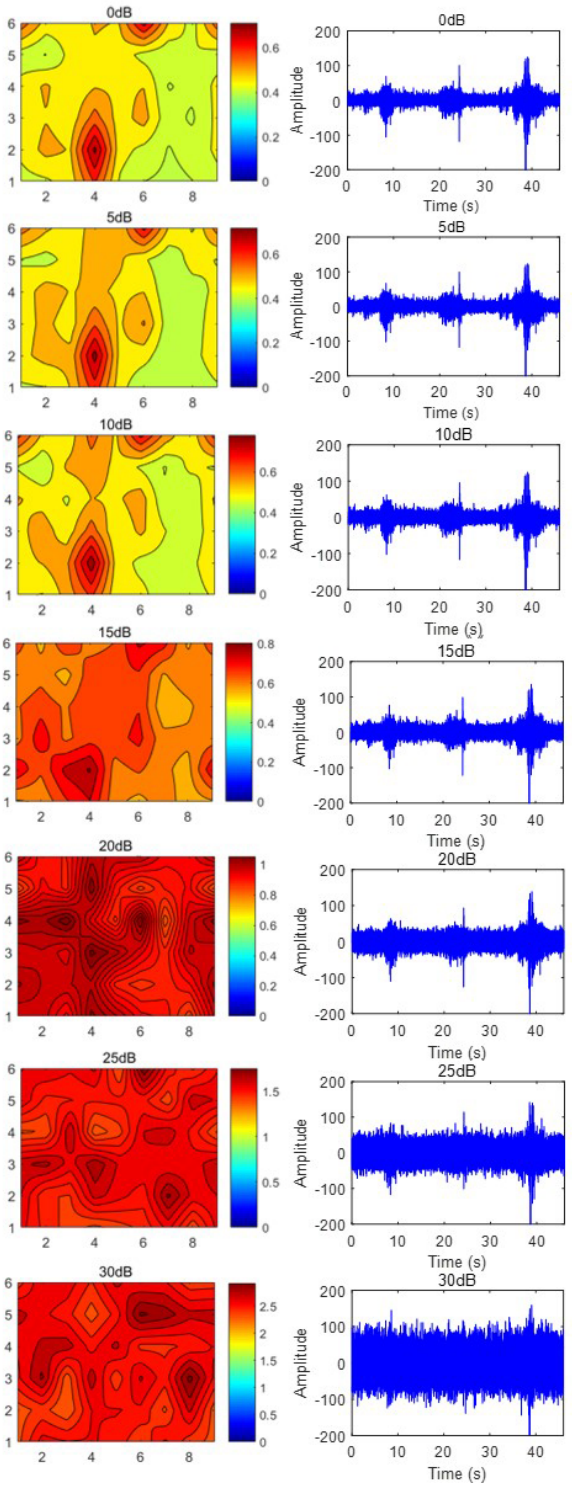

FIGURE 3. Visualization of the EMG at different noise levels. (A) Variation of EMG topographic map, the former 48 channels of pre-processed EMG signals corresponding to "hand close" for ST05 were used. (B) EMG amplitude variation, the 46th channel of preprocessed EMG signals corresponding to "hand close" for ST05 were considered.

classifier combinations in the following context to assess their tolerance to WGN interference in the subsequent analyses. Another four optimal feature-classifier combinations including the LDA-TDAR, KNN-TD4, RF-TD4, and

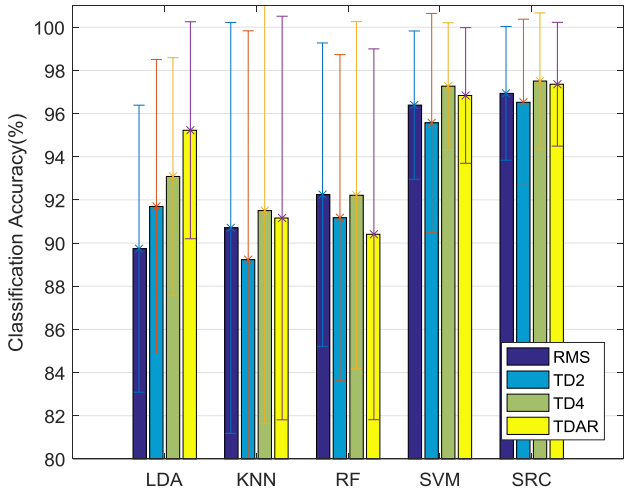

FIGURE 4. Classification performance of all feature-classifier combinations in the absence of WGN corruption.

TABLE 1. Average cost time for SRC when using different feature sets.

Feature Set	Cost Time (s)	Pairwise comparison	*p-value*
RMS	21.72±5.00	--	--
TD2	26.12±5.04	RMS VS TD2	0.18
TD4	28.92±5.51	RMS VS TD4	0.003
TDAR	37.46±7.19	RMS VS TDAR	0.001

SVM-TD4 were selected due to their highest classification accuracies among all the other feature sets for each classifier. Noting among all the five optimal feature-classifier combinations, the average classification accuracy of the proposed RMS-SRC scheme is 96.94%, only 0.33% lower than that when using TD4-SVM, but significantly higher than those of the TDAR-LDA, TD4-KNN, and TD4-RF according to the paired t-test ($p\text{-}value < 0.05$), with increased accuracy of 1.72%, 5.44%, and 4.72%, respectively.

C. CLASSIFICATION PERFORMANCE WITH NOISE ON ALL EMG RECORDINGS

The tolerance of the proposed RMS-SRC scheme and the other optimal feature-classifier combinations was then analyzed by introducing varying levels of WGN into the entire EMG recordings (FIGURE 5). It can be observed that the classification accuracy of all the five examined feature-classifier combinations was stable when the SNR of additive WGN was less than or equal to 15 dB (<=15 dB), which suggest that all the pattern-recognition schemes are robust to noise contaminations within a limited range. However, when the SNR of the additive WGN level increased to 20 dB, the classification accuracy was significantly reduced for all pattern-recognition schemes except for the TD4-KNN ($p\text{-}value < 0.01$). And the classification accuracy continued to reduce dramatically when the SNR level increased to 25dB and 30dB ($p\text{-}value < 0.01$). Noting the TD4-SVM and RMS-SRC achieved consistently higher average classification accuracy than the other three pattern recognition schemes with respect to each noise level, and the RMS-SRC began to outperform TD4-SVM when the SNR of noise reached 20 dB with higher and concentrated classification accuracy. These findings indicate that the proposed RMS-SRC scheme would be more robust to WGN contamination that are inevitably inherent in most EMG recordings.

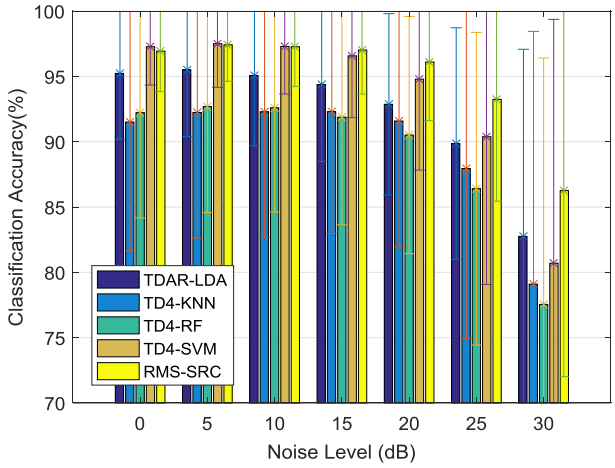

FIGURE 5. Classification performance of five optimal feature-classifier combinations with noise on all EMG recordings.

The classification performance of all the SRC-based pattern-recognition schemes were also included for comparison (FIGURE 6). Their classification accuracies reduced dramatically when the SNR level increased to 25dB and 30dB ($p\text{-}value < 0.01$). It is noteworthy that the RMS-SRC kept high classification accuracy, only slightly lower than that of the TD4-SRC and TDAR-SRC ($p\text{-}value > 0.05$).

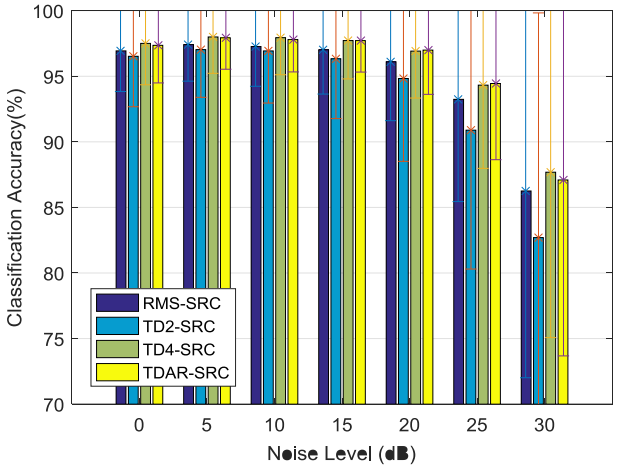

FIGURE 6. Classification performance of all SRC-based feature-classifier combinations with noise on all EMG recordings.

D. CLASSIFICATION PERFORMANCE WITH NOISE ON PARTIAL EMG RECORDINGS

By introducing WGN of varying levels into either the training EMG or the testing data, the robustness of the five pattern

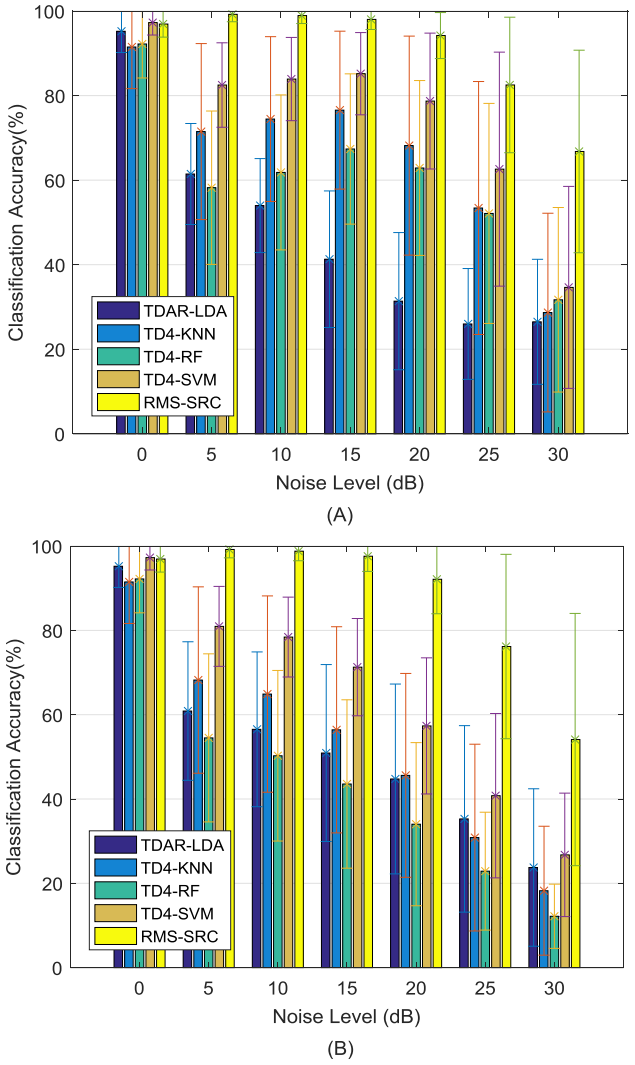

FIGURE 7. Classification performance of five optimal feature-classifier combinations with noise on partial EMG recordings. The WGN was added to training set (A) and testing set (B), respectively.

recognition schemes were assessed. FIGURE 7 demonstrates the average classification accuracy (mean± standard deviation) among all subjects when the training set (80% of the EMG recordings, FIGURE 7(A)) and testing set (20% of the EMG recordings, FIGURE 7(B)) were corrupted by WGN, respectively, the five optimal feature-classifier combinations were considered.

It is found that for both contamination cases, the partial noise degraded the classification performance dramatically when using TDAR-LDA, TD4-KNN, TD4-RF, and TD4-SVM ($p\text{-}value < 0.01$). However, the classification accuracy of the proposed RMS-SRC scheme retained high mean accuracy which was above 92% when the SNR of WGN reached 20 dB. Moreover, the statistical analysis indicates that the proposed RMS-SRC scheme significantly outperformed the other four pattern recognition schemes irrespective of the SNR of WGN ($p\text{-}value < 0.01$). Specifically, when the SNR of WGN was within 20 dB, the difference value between the average classification accuracy of TD4-SVM and that of RMS-SRC ranged from 12.60% to 16.96% when the training set was contaminated, and from 18.24% to 34.79% when the testing set was contaminated.

We further explored the robustness of all SRC-based feature-classifier combinations in the presence of partial WGN interference (FIGURE 8). It is observed that the RMS outperformed the other feature sets regardless of the level of WGN when 20% of the EMG recordings were contaminated (FIGURE 8(B)). And in the case of 80% contaminated EMG recordings, the RMS-SRC achieved almost the same accuracy with that of TDAR-SRC (FIGURE 8(A)). These outcomes suggest that the RMS with only one dimensionality is sufficient for the SRC to bring a high and robust classification performance.

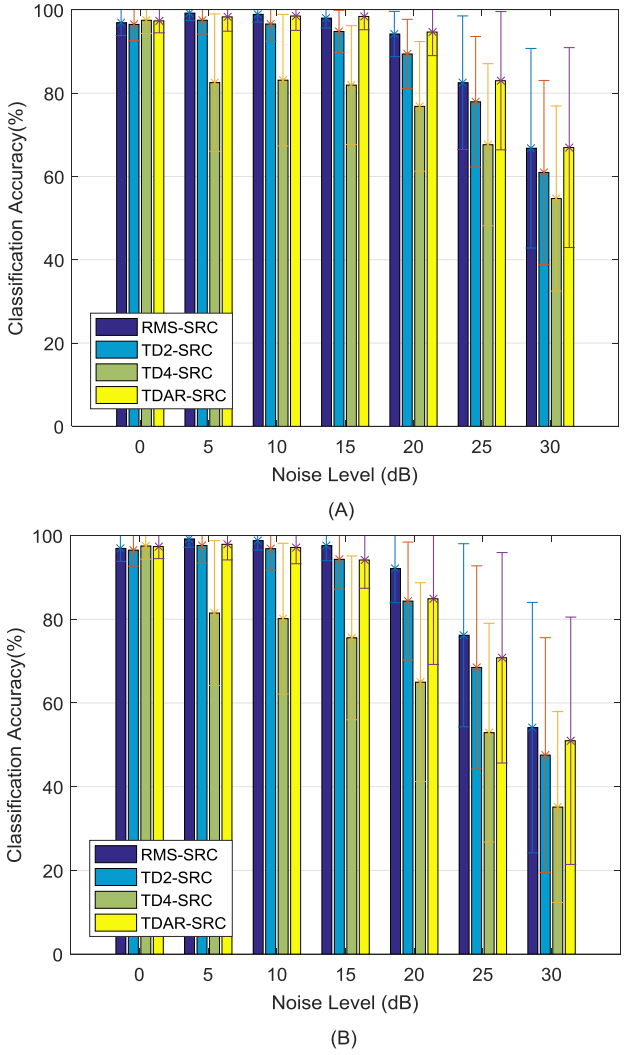

FIGURE 8. Classification performance of all four SRC-based feature-classifier combinations with noise on partial EMG recordings. The WGN was added to training set (A) and testing set (B), respectively.

IV. DISCUSSION AND CONCLUSIONS

Surface EMG signals are often contaminated by WGN and such noise would inevitably influence the performance of EMG-PR system. The intermittent characteristic of

WGN during long-term EMG recordings makes it difficult to attenuate the noise in real-time by means of the currently available denoising approaches. Aiming at providing an accurate, stable, and robust EMG-PR system that is highly invariant to the interference of WGN, a RMS-SRC based pattern recognition scheme is proposed in this study. The results show that in comparison to the other four pattern recognition schemes including TDAR-LDA, TD4-KNN, TD4-RF, and TD4-SVM, the RMS-SRC achieved similar classification accuracy in the presence of limited noise contamination (0-15 dB) on all EMG recordings, and significantly outperformed the abovementioned schemes as the SNR of WGN increased (20-30 dB). Moreover, the proposed RMS-SRC scheme significantly outperformed the other four examined pattern recognition schemes when the WGN existed in either training set or testing set only. These outcomes suggest the comparative advantage of the proposed RMS-SRC scheme over the other commonly used pattern recognition schemes in myoelectric control.

In current study, the optimal feature-classifier combinations were selected in terms of classification accuracy and the required time to make decision. The average cost time for the proposed RMS-SRC scheme was observed to be approximately 21.7 ms, which is significantly longer than the values obtained when using the other feature-classifier combinations (excluding that with SRC). With the development of the CPU or GPU, we believe that the consumption cost of the optimum SRC algorithms will be sharply decreased in the future.

In the absence of WGN, we further examined if there is interaction effect of feature set and classifier by means of two-way ANOVA statistical analysis, and the results showed that the classification accuracy was significantly affected by classifiers ($p\text{-}value < 0.01$) rather than the four different feature sets ($p\text{-}value = 0.38$). According to FIGURE 4, however, the average classification accuracy of LDA seems closely related with the selection of feature sets, while the other classifiers were not highly sensitive to the selection of feature sets (with difference value of about 2% between the highest and the lowest classification accuracy). These outcomes may be attributed to the different principles upon which the classification schemes were built. Specifically, the LDA is to determine a subspace projection that maximizes the distance between class data clusters while minimizing the scatter of each cluster, and appropriate increase of the dimensionality of feature matrix would make the clusters affiliated to different classes more separable in the high-dimensional space. Therefore, the increased dimensionality of the feature matrix (from 1 to 2, 4, and 8, respectively) resulted in higher classification accuracy in the current study. When using KNN, the similarity between the observed data and training set was measured with Euclidean distance metric, which maybe insufficient to discriminate two close clusters in a high-dimensional space, thus its classification accuracies with respect to the RMS, TD2, TD4, and TDAR feature were approximately the same. When using SVM, the RMS feature matrix obtained from HD-EMG may be sufficient to obtain support hyper-planes with maximum distance so as to properly discriminate a specific class from the other classes. Meanwhile, the SRC which is based on the concept that patterns from the same class lie on a sparse linear subspace, and the RMS feature matrix that has same dimensionality to the HD-EMG might be sufficient to span a subspace for accurate projection of the test vector, and thus the dimensionality variation of patterns would not affect the projection accuracy significantly [34], [36].

By comparing the results in FIGURE 4 and FIGURE 7, it is found that the KNN began to outperform RF in the presence of partial WGN interference, while RF was better than KNN in the absence of WGN. The incapability of Euclidean distance metric to discriminate two clusters when using KNN might account for this result. Specifically, the zero crossing, wave length, and slope sign changes in TD4 feature set are sensitive to changes in EMG waveform according to their definitions. And for this reason, the higher the SNR of WGN is, the more difference there would be between the training set and the testing set when either set was contaminated by WGN. However, the Euclidean distance metric of KNN might be insufficient to identify the contaminated cluster from the clean cluster even though which belong to the same class.

An important finding in the current study is that the proposed RMS-SRC pattern recognition scheme was highly tolerant to WGN interferences (FIGURE 5-FIGURE 8), particularly in the condition of a small part of WGN contamination (FIGURE 7(B) and FIGURE 8 (B)). There might be two main reasons accounting for this outcome. First, the RMS is robust to noise interference due to its lowest dimensionality (FIGURE 8 (B)). The dimensional increase of EMG features when using other more complex feature sets could provide more information for characterizing EMG patterns, and thereby leading to higher classification accuracy for LDA (FIGURE 4). However, for a specific motion that was contaminated in either the training stage or testing stage, the disparities of the corresponding EMG patterns would be increased if higher dimensional feature sets are utilized. In contrast, the RMS feature with only one dimensionality has the advantage of tolerance to the disparities. The second possible reason accounting for the significantly better classification performance of the proposed RMS-SRC scheme is that the SRC algorithm has better robustness to noise corruption in comparison to the other classical classifiers. That is, the errors due to noise contamination are sparse with respect to the standard basis (raw HD-EMG recordings), and the theory of sparse representation could handle such errors well [35], [36].

With the aim of developing a simple and robust practical myoelectric control paradigm for the robot-based neurorehabilitation system, this study provides a promising pattern recognition scheme, RMS-SRC for myoelectric controlled systems. This proposed scheme has an obvious comparative advantage to the commonly used classification schemes in terms of classification accuracy. More notably, the utilization of the RMS-SRC could improve the robustness of

EMG-PR system against intermittent noises associated with long-term practical use in real life. In the future, we hope to further improve the computation speed of the SRC algorithm by utilizing other optimization algorithms to solve the optimal L1-minimization problem. Additionally, our future study will focus on integrating the proposed RMS-SRC scheme into a real-time EMG-PR platform to examine its reliability in real-time, and its robustness to untrained effect of electrode shift, variation of muscle contraction force, and limb position variation.

ACKNOWLEDGEMENT

The authors would like to thank the subjects who participated in this study, assistant research fellow Wanhua Lin and Haoshi Zhang, PhD student Pinggao Huang for their technical assistance, and physiotherapists Tianbao Sun, Zhenhui Yang for their assistance in data acquisition experiment.

REFERENCES

[1] D. Farina *et al.*, "The extraction of neural information from the surface EMG for the control of upper-limb prostheses: Emerging avenues and challenges," *IEEE Trans. Neural Syst. Rehabil. Eng.*, vol. 22, no. 4, pp. 797–809, Jul. 2014.

[2] B. Peerdeman *et al.*, "Myoelectric forearm prostheses: State of the art from a user-centered perspective," *J. Rehabil. Res. Develop.*, vol. 48, no. 6, pp. 719–737, 2011.

[3] N. Jiang, S. Dosen, K.-R. Müller, and D. Farina, "Myoelectric control of artificial limbs—Is there a need to change focus? [In the spotlight]," *IEEE Signal Process. Mag.*, vol. 29, no. 5, pp. 150–152, Sep. 2012.

[4] Z. Lu, K.-Y. Tong, H. Shin, S. Li, and P. Zhou, "Advanced myoelectric control for robotic hand-assisted training: Outcome from a stroke patient," *Frontiers Neurol.*, vol. 8, p. 107, Mar. 2017.

[5] A. Ramos-Murguialday *et al.*, "Decoding upper limb residual muscle activity in severe chronic stroke," *Ann. Clin. Transl. Neurol.*, vol. 2, no. 1, pp. 1–11, Jan. 2015.

[6] M. Rojas-Martínez, M. A. Mañanas, J. F. Alonso, and R. Merletti, "Identification of isometric contractions based on high density EMG maps," *J. Electromyogr. Kinesiol.*, vol. 23, no. 1, pp. 33–42, 2013.

[7] X. Zhang and P. Zhou, "High-density myoelectric pattern recognition toward improved stroke rehabilitation," *IEEE Trans. Biomed. Eng.*, vol. 59, no. 6, pp. 1649–1657, Jun. 2012.

[8] S. W. Lee, K. M. Wilson, B. A. Lock, and D. G. Kamper, "Subject-specific myoelectric pattern classification of functional hand movements for stroke survivors," *IEEE Trans. Neural Syst. Rehabil. Eng.*, vol. 19, no. 5, pp. 558–566, Oct. 2011.

[9] Z. Lu, X. Chen, X. Zhang, K.-Y. Tong, and P. Zhou, "Real-time control of an exoskeleton hand robot with myoelectric pattern recognition," *Int. J. Neural Syst.*, vol. 27, no. 5, p. 1750009, Aug. 2017.

[10] Y. Geng, X. Zhang, Y.-T. Zhang, and G. Li, "A novel channel selection method for multiple motion classification using high-density electromyography," *Biomed. Eng. Online*, vol. 13, p. 102, Jul. 2014.

[11] Z. O. Khokhar, Z. G. Xiao, and C. Menon, "Surface EMG pattern recognition for real-time control of a wrist exoskeleton," *Biomed. Eng. Online*, vol. 9, p. 41, Aug. 2010.

[12] C. J. De Luca, L. D. Gilmore, M. Kuznetsov, and S. H. Roy, "Filtering the surface EMG signal: Movement artifact and baseline noise contamination," *J. Biomech.*, vol. 43, no. 8, pp. 1573–1579, 2010.

[13] P. McCool, L. Petropoulakis, J. J. Soraghan, and N. Chatlani, "Improved pattern recognition classification accuracy for surface myoelectric signals using spectral enhancement," *Biomed. Signal Process. Control*, vol. 18, pp. 61–68, Apr. 2015.

[14] X. Zhang and P. Zhou, "Filtering of surface EMG using ensemble empirical mode decomposition," *Med. Eng. Phys.*, vol. 35, no. 4, pp. 537–542, 2013.

[15] H. Rehbaum and D. Farina, "Adaptive common average filtering for myocontrol applications," *Med. Biol. Eng. Comput.*, vol. 53, no. 2, pp. 179–186, Feb. 2015.

[16] J. Maier, A. Naber, and M. Ortiz-Catalan, "Improved prosthetic control based on myoelectric pattern recognition via wavelet-based de-noising," *IEEE Trans. Neural Syst. Rehabil. Eng.*, vol. 26, no. 2, pp. 506–514, Feb. 2018.

[17] J. M. Hahne, B. Graimann, and K.-R. Müller, "Spatial filtering for robust myoelectric control," *IEEE Trans. Biomed. Eng.*, vol. 59, no. 5, pp. 1436–1443, May 2012.

[18] H. Huang, P. Zhou, G. L. Li, and T. Kuiken, "Spatial filtering improves EMG classification accuracy following targeted muscle reinnervation," *Ann. Biomed. Eng.*, vol. 37, no. 9, pp. 1849–1857, Sep. 2009.

[19] A. Phinyomark, R. N. Khushaba, E. Ibáñez-Marcelo, A. Patania, E. Scheme, and G. Petri, "Navigating features: A topologically informed chart of electromyographic features space," *J. The Roy. Soc. Interface*, vol. 14, no. 137, p. 20170734, Dec. 2017.

[20] R. N. Khushaba, M. Takruri, J. V. Miro, and S. Kodagoda, "Towards limb position invariant myoelectric pattern recognition using time-dependent spectral features," *Neural Netw.*, vol. 55, pp. 42–58, Jul. 2014.

[21] J. He, D. Zhang, X. Sheng, S. Li, and X. Zhu, "Invariant surface EMG feature against varying contraction level for myoelectric control based on muscle coordination," *IEEE J. Biomed. Health Inform.*, vol. 19, no. 3, pp. 874–882, Jun. 2014.

[22] R. N. Khushaba, A. H. Al-Timemy, A. Al-Ani, and A. Al-Jumaily, "A framework of temporal-spatial descriptors-based feature extraction for improved myoelectric pattern recognition," *IEEE Trans. Neural Syst. Rehabil. Eng.*, vol. 25, no. 10, pp. 1821–1831, Oct. 2017.

[23] A. Phinyomark, C. Limsakul, and P. Phukpattaranont, "A novel feature extraction for robust EMG pattern recognition," *J. Comput.*, vol. 1, no. 1, pp. 71–80, 2009.

[24] S.-H. Park and S.-P. Lee, "EMG pattern recognition based on artificial intelligence techniques," *IEEE Trans. Rehabil. Eng.*, vol. 6, no. 4, pp. 400–405, Dec. 1998.

[25] T. A. Kuiken *et al.*, "Targeted muscle reinnervation for real-time myoelectric control of multifunction artificial arms," *J. Amer. Med. Assoc.*, vol. 301, pp. 619–628, Feb. 2009.

[26] Y. Geng, P. Zhou, and G. Li, "Toward attenuating the impact of arm positions on electromyography pattern-recognition based motion classification in transradial amputees," *J. Neuroeng. Rehabil.*, vol. 9, p. 74, Oct. 2012.

[27] K. Nazarpour, A. R. Sharafat, and S. M. P. Firoozabadi, "Application of higher order statistics to surface electromyogram signal classification," *IEEE Trans. Biomed. Eng.*, vol. 54, no. 10, pp. 1762–1769, Oct. 2007.

[28] Y. Huang, K. B. Englehart, B. Hudgins, and A. D. C. Chan, "A Gaussian mixture model based classification scheme for myoelectric control of powered upper limb prostheses," *IEEE Trans. Biomed. Eng.*, vol. 52, no. 11, pp. 1801–1811, Nov. 2005.

[29] F. H. Y. Chan, Y.-S. Yang, F. K. Lam, Y.-T. Zhang, and P. A. Parker, "Fuzzy EMG classification for prosthesis control," *IEEE Trans. Rehabil. Eng.*, vol. 8, no. 3, pp. 305–311, Sep. 2000.

[30] A. B. Ajiboye and R. F. Weir, "A heuristic fuzzy logic approach to EMG pattern recognition for multifunctional prosthesis control," *IEEE Trans. Neural Syst. Rehabil. Eng.*, vol. 13, no. 3, pp. 280–291, Sep. 2005.

[31] Z. Li, B. Wang, C. Yang, Q. Xie, and C.-Y. Su, "Boosting-based EMG patterns classification scheme for robustness enhancement," *IEEE J. Biomed. Health Inform.*, vol. 17, no. 3, pp. 545–552, May 2013.

[32] R. Su, X. Chen, S. Cao, and X. Zhang, "Random forest-based recognition of isolated sign language subwords using data from accelerometers and surface electromyographic sensors," *Sensors*, vol. 16, no. 1, p. 100, Jan. 2016.

[33] M. A. Oskoei and H. Hu, "Support vector machine-based classification scheme for myoelectric control applied to upper limb," *IEEE Trans. Biomed. Eng.*, vol. 55, no. 8, pp. 1956–1965, Aug. 2008.

[34] L. Zhang, M. Yang, and X. Feng, "Sparse representation or collaborative representation: Which helps face recognition?" in *Proc. Int. Conf. Comput. Vis.*, Nov. 2011, pp. 471–478.

[35] J. Wright, Y. Ma, J. Mairal, G. Sapiro, T. S. Huang, and S. Yan, "Sparse representation for computer vision and pattern recognition," *Proc. IEEE*, vol. 98, no. 6, pp. 1031–1044, Jun. 2010.

[36] J. Wright, A. Y. Yang, A. Ganesh, S. S. Sastry, and Y. Ma, "Robust face recognition via sparse representation," *IEEE Trans. Pattern Anal. Mach. Intell.*, vol. 31, no. 2, pp. 210–227, Feb. 2009.

[37] C. Lin, B. Wang, X. Zhao, and M. Pang, "Optimizing kernel PCA using sparse representation-based classifier for MSTAR SAR image target recognition," *Math. Problems Eng.*, vol. 2013, Apr. 2013, Art. no. 847062.

[38] O. W. Samuel *et al.*, "Pattern recognition of electromyography signals based on novel time domain features for amputees' limb motion classification," *Comput. Elect. Eng.*, vol. 67, pp. 646–655, Apr. 2018.
[39] B. Hudgins, P. Parker, and R. N. Scott, "A new strategy for multifunction myoelectric control," *IEEE Trans. Biomed. Eng.*, vol. 40, no. 1, pp. 82–94, Jan. 1993.
[40] D. Graupe and W. K. Cline, "Functional separation of EMG signals via ARMA identification methods for prosthesis control purposes," *IEEE Trans. Syst., Man, Cybern.*, vol. SMC-5, no. 2, pp. 252–259, Mar. 1975.
[41] X. Chen and Z. J. Wang, "Pattern recognition of number gestures based on a wireless surface EMG system," *Biomed. Signal Process. Control*, vol. 8, no. 2, pp. 184–192, Mar. 2013.
[42] Y. Geng, O. W. Samuel, Y. Wei, and G. Li, "Improving the robustness of real-time myoelectric pattern recognition against arm position changes in transradial amputees," *Biomed Res. Int.*, vol. 2017, Apr. 2017, Art. no. 5090454.
[43] L. Breiman, "Random forests," *Mach. Learn.*, vol. 45, no. 1, pp. 5–32, 2001.
[44] V. Svetnik, A. Liaw, C. Tong, J. C. Culberson, R. P. Sheridan, and B. P. Feuston, "Random forest: A classification and regression tool for compound classification and QSAR modeling," *J. Chem. Inf. Comput. Sci.*, vol. 43, no. 6, pp. 1947–1958, 2003.
[45] D. R. Cutler *et al.*, "Random forests for classification in ecology," *Ecology*, vol. 88, no. 11, pp. 2783–2792, 2007.
[46] C.-C. Chang and C.-J. Lin, "LIBSVM: A library for support vector machines," *ACM Trans. Intell. Syst. Technol.*, vol. 2, Apr. 2011, Art. no. 27.

YANJUAN GENG (M'12) received the Ph.D. degree in pattern recognition and intelligent system from the University of Chinese Academy of Sciences, Beijing, China, in 2014. She is currently an Assistant Professor with the Research Centre for Neural Engineering, Institute of Biomedical and Health Engineering, Shenzhen Institutes of Advanced Technology, Chinese Academy of Sciences, China. Her research interests include the myoelectric control of powered prosthesis and rehabilitation for the hemiparesis.

YATAO OUYANG is currently a Professor of medicine and the Vice Director of the Guangdong Provincial Work Injury Rehabilitation Center. His research interests mainly focus on the physical therapy, occupation therapy, and myoelectric prosthesis.

OLUWAROTIMI WILLIAMS SAMUEL (M'18) received the Ph.D. degree in pattern recognition and intelligent systems from the University of Chinese Academy of Sciences in 2018. He is currently a Post-Doctoral Research Fellow with the Research Centre for Neural Engineering, Institute of Biomedical and Health Engineering, Shenzhen Institutes of Advanced Technology, Chinese Academy of Sciences, China. His research interests include rehabilitation robotics, biomedical signal processing, machine learning, and clinical decision support systems, among others.

SHIXIONG CHEN (M'12) received the Ph.D. degree in speech and hearing science from Arizona State University, USA, in 2012. He is currently an Associate Professor with the Research Centre for Neural Engineering, Institute of Biomedical and Health Engineering, Shenzhen Institutes of Advanced Technology, Chinese Academy of Sciences, China. His current research interests include mechanics of hearing, otoacoustic emissions, inner ear nonlinearity, hearing loss detection, and rehabilitation of hearing disorders.

XIAOQIANG LU (M'14–SM'15) is currently a Full Professor with the Center for Optical Imagery Analysis and Learning, Xi'an Institute of Optics and Precision Mechanics, Chinese Academy of Sciences, Xi'an, China. His research interests include pattern recognition, machine learning, hyperspectral image analysis, cellular automata, and medical imaging.

CHUANG LIN (M'14) received the Ph.D. degree in signal processing from the Harbin Institute of Technology, Harbin, China, in 2008. He is currently an Associate Professor with the CAS Key Laboratory of Human-Machine Intelligence-Synergy Systems, Research Center for Neural Engineering, Institute of Biomedical and Health Engineering, Shenzhen Institutes of Advanced Technology, Chinese Academy of Sciences. His research interests include biomedical signal processing, pattern recognition, and machine learning.

GUANGLIN LI (M'01–SM'06) received the Ph.D. degree in biomedical engineering from Zhejiang University, Hangzhou, China, in 1997. He is currently a Full Professor with the Research Centre for Neural Engineering, Shenzhen Institute of Advanced Technology, Chinese Academy of Sciences, Shenzhen, China. His research interests include neuroprostheses, neural–machine interfaces, biomedical signal analysis, and computational biomedical engineering.